ChemComm

ROYAL SOCIETY OF CHEMISTRY

COMMUNICATION

View Article Online
View Journal | View Issue

Cite this: *Chem. Commun.*, 2025, **61**, 16242

Received 25th April 2025,
Accepted 7th September 2025

DOI: 10.1039/d5cc02304a

rsc.li/chemcomm

Curcumin-based-fluorescent staining and microfluidic detection of microplastics in wastewater effluent

Juviya Mathew,[a] Haider Warraich,[b] Ratul Kumar Das,[a] Pouya Rezai[b] and Satinder Kaur Brar*[a]

We present a fast, eco-friendly method for detecting polyethylene microplastics (<10 μm) in wastewater effluent using curcumin as a natural fluorescent dye. Curcumin-stained particles exhibited strong green fluorescence and electrophoretic capture in a microfluidic device, demonstrating a sustainable alternative to synthetic dyes for environmental microplastic detection.

The pervasiveness of microplastics (MPs) as emerging pollutants in aquatic and terrestrial ecosystems has adverse effects on both the environment and living organisms.[1] Due to their small size, ranging from 1 μm to 5 mm, the detection and characterization of MPs are challenging.[2] This complicates the studies to determine their distribution, composition, and ecotoxicity. However, detection and quantification of MPs is crucial to assess their distribution within the different environmental matrices and the potential hazards they pose within the ecosystem.[3] One of the most effective, low-cost and fastest tools for the visual detection of MPs is by fluorescent staining.[4] This is a promising technique to detect MPs accumulated in terrestrial and aquatic invertebrates[5] and MPs present in different environmental samples.[6] Fluorescent staining is also useful for assessing the surface modifications on MPs persistent in environmental matrices with time and their hydrodynamic studies.[7] The history of fluorescent staining of MPs and the different types of fluorescent dyes used for the detection of MPs so far and their characteristics are discussed in Fig. S1 and Table S1, respectively. Among them, the most widely adopted fluorescent dye has been Nile Red since 2010.[8,9] However, Nile Red is a lipophilic fluorescent dye that exhibits strong solvatochromic behaviour, which shifts fluorescence emission from yellow to red with the change in the polarity of the MPs.[10] It also leaches out easily from the surface of MPs, limiting tracking, and can cause potential ecological risks to living organisms.[11] Therefore, there is a need for natural dyes that can stain MPs efficiently and mitigate the risk of secondary pollution. In this context, curcumin can be an effective fluorescent dye for MP detection in environmental samples. Moreover, fluorescent dyeing of MPs with curcumin promotes an eco-friendly alternative for detection by preventing the release of secondary harmful contaminants, which supports sustainable development goals (SDGs) 6 & 14 of the United Nations. Unlike many synthetic dyes used for MP staining that contain carcinogens or endocrine disruptors that affect human health, curcumin is an edible and biocompatible fluorescent dye. The use of this dye benefits both the workers in the dyeing industry and consumers (SDG 3). Being a plant-based fluorescent dye, curcumin has a lower carbon footprint, helping combat climate change (SDG 13). A comparative summary of the key differences between Nile Red and curcumin is provided in the SI (Table S2). Curcumin is a yellow polyphenolic compound and the major ingredient in turmeric (*Curcuma longa* L.). It has a wide spectrum of biological and pharmacological properties, including antioxidant and anticarcinogenic properties, and is generally recognized as safe (GRAS) by the Food and Drug Administration (FDA, USA) when used as a food additive.[12] Curcumin was also used for delivery to cancer cells by a nano formulation with a tri-component polymeric composite.[13] It generally exhibits a very weak solvatochromic effect because its molecular structure does not readily facilitate significant charge separation upon excitation.[14] Thus, the polarity of the molecule does not change drastically when transitioning to an excited state, which is the key mechanism behind solvatochromism. In addition, its intramolecular hydrogen bonding network limits solvent interactions that hinder significant shifts in absorption spectra based on the polarity of the solvent.[15] This in fact is advantageous for MP detection as it interacts minimally with the surrounding solvent environment and reduces background signals. Thereby, it enhances its specificity for labelling MPs by improving contrast and making MPs more distinguishable during the detection process. Curcumin has a high fluorescent quantum yield and emits in the visible range, *i.e.* at 571 nm.[16] This provides brighter and more distinguishable images under the standard fluorescence microscopy settings. This article thus explores the potential of curcumin as an effective and eco-friendly approach for

[a] *Department of Civil Engineering, Lassonde School of Engineering, York University, Toronto, Canada. E-mail: satinder.brar@lassonde.yorku.ca*
[b] *Department of Mechanical Engineering, Lassonde School of Engineering, York University, Toronto, Canada. E-mail: prezai@yorku.ca*

fluorescent staining of MPs. This novel staining approach can be used for the quantification of MPs in different aqueous matrices like freshwater, marine, wastewater (WW), soil and sediments.

Existing analytical techniques, such as micro-Fourier Transform Infrared (μ-FTIR) and μ-Raman spectroscopy, as well as mass spectrometric instruments, are expensive, and require high operational costs and extensive human labour.[2] Thermal techniques such as differential scanning calorimetry (DSC) and pyrolysis–gas chromatography–mass spectrometry (Py-GC-MS) are destructive in nature.[2] These advanced techniques typically detect MPs down to 1 μm in size; however, matrix-assisted laser desorption/ionization–time-of-flight mass spectrometry (MALDI-TOF) detected MPs in the size range of 200–400 nm, but remains prohibitively expensive[17] (Table S3). Owing to this complexity, microfluidic devices are a promising alternative for the low-cost, point-of-need (PoN) detection of MPs. Curcumin staining enables both the optical detection of MPs and modification of their surface charge, inducing electrophoretic mobility that supports electrical detection. Leveraging this property, we adapted a simple, low-cost microfluidic sensor previously reported by Rezai *et al.* (2022)[18] to test its feasibility for the WW final effluent. MPs of size <1 μm can easily escape primary and secondary treatment stages of WW treatment and flow into freshwater sources through the final effluent.[2] Polyethylene (PE), the most frequently detected MP in environmental samples, was chosen as a representative material. PE particles (200–9900 nm) were stained with curcumin, spiked into the WW effluent, and analyzed using the device. The weak solvatochromic effect of curcumin minimizes interference from the aqueous environment, thereby improving contrast and detectability. This study serves as a proof-of-concept, presenting the first demonstration of curcumin-stained MPs detected in a microfluidic system using both fluorescence and electrical techniques. This approach reduces analysis time and reagent use compared to conventional methods, providing a sustainable basis for future refinement and broader application.

The microscopic analysis of PE MPs before and after curcumin-staining is shown in Fig. 1. The virgin PE-A MPs had a glassy-like appearance under a stereomicroscope, while PE-B MPs appeared as transparent beads. After curcumin staining, both PE-A and PE-B had a yellow stain on their surfaces after treating them with curcumin for 24 hours. Curcumin-stained PE-A MPs dispersed in Milli-Q and the PE-B MPs beads were used for fluorescence microscopic analysis. Under blue light excitation wavelength (467 nm), both MPs emitted green fluorescence and confirmed successful staining of MPs with curcumin regardless of their size range. Upon addition of the solvent methanol to the curcumin-stained PE MPs, the yellow stain on the surface easily dissolved into methanol, forming a yellow solution. The destained PE-A MPs were observed to have the same glassy-like appearance as the virgin PE-A MPs. Similarly, PE-B MPs had a transparent bead-like appearance after the destaining process. This confirmed that curcumin-stained PE MPs can be easily destained using methanol. Methanol was selected for staining and destaining because of its optimal polarity and superior curcuminoid extraction efficiency.[19] Further justification is provided in the SI (Section I (B)).

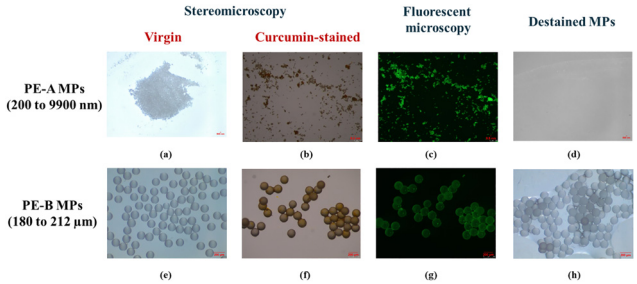

Fig. 1 Microscopic images of (a) and (e) virgin, (b) and (f) curcumin-stained, (c) and (g) fluorescent microscopic images and (d) and (h) destained PE-A and PE-B MPs. *PE-Polyethylene, MPs-microplastics.

This was further confirmed by the UV-Visible analysis of the extracted curcumin from the stained MPs into methanol (Fig. S6). The absorbance peak (λ_{max}) of curcumin was intact at 420 nm before and after staining, which proved that MPs can be easily recovered after staining with curcumin (see the SI, Section II(C)). The effect of concentration of curcumin in methanol on the fluorescent staining is shown in Fig. S7 and Table S5.

As observed in Fig. 2, the FTIR analysis of curcumin in methanol showed the characteristic peaks at 3334 cm^{-1} and 2974 cm^{-1} corresponding to the stretching vibrations of aromatic –OH groups and C–H bonds, respectively. The absorption bands at 1232 cm^{-1} and 1038 cm^{-1} matched C–O stretch of phenyl alkyl ether. In addition, the absorption band at 658 cm^{-1} was out of phase C–O stretch of the aromatic ring.[20] The FTIR spectroscopy of both the stained PE-A and PE-B MPs showed the characteristic bands of each functional group in the structure of virgin PE MPs. The absorption peak at 2916 cm^{-1}, a characteristic of CH_2 asymmetric stretching, remained unaltered in the spectrum of the stained PE-A and PE-B MPs. Similarly, the peak at 2848 cm^{-1}, attributable to CH_2 symmetric stretching, was consistent after staining. The bending vibrations of CH_2 at 1473 cm^{-1} and the rocking motions at 719 cm^{-1} also

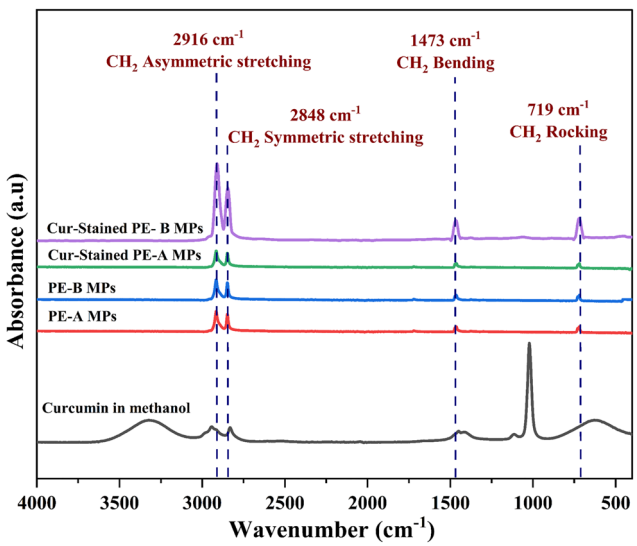

Fig. 2 FTIR analysis of PE-A and PE-B MPs before and after staining. *PE: polyethylene; MPs: microplastics; Cur: curcumin.

showed no discernible changes.[21] The stability of these peaks suggested that the curcumin staining process did not induce any chemical changes to PE MPs regardless of their size and electrostatic interactions occurred between curcumin and PE MPs, which supported the destaining results.

Curcumin exhibited excellent fluorescence under slightly basic conditions (pH 7 to 8) with excellent encapsulation efficiency.[22] Curcumin does not carry a charge at pH 7 to 8, which favoured PE-A MPs to retain their negative zeta potential. This further supported the destaining process as confirmed by UV-vis and FTIR analyses, where only electrostatic interactions were observed between the curcumin stain and PE MPs. Thus, curcumin-staining could give a strong fluorescence signal, which could assist in easier identification of MPs in real environmental water matrices, which have pH values ranging from 7 to 8. The pH analysis of the samples is shown in Table S6.

The zeta potential values of the water samples, and virgin and curcumin-stained PE-A MPs, are shown in Table S7. Only PE-A MPs can be studied as the maximum particle size for zeta potential measurements is 100 μm. Both the virgin and curcumin-stained PE-A MPs are negatively charged *i.e.* -38 ± 4.35 mV and -25.6 ± 4.02 mV in Milli-Q and *i.e.* -24 ± 7.01 mV to -22.5 ± 6.88 mV in the WW final effluent, respectively. This showed the successful adsorption of curcumin onto the surfaces of PE-A MPs. The layer of curcumin adsorbed on the surface of the PE-A MPs decreased the negative charge of their virgin form by 12 mV in Milli-Q and only by 1.5 mV in the WW final effluent. As observed in Table S7, the conductivity of the Milli-Q spiked with virgin and curcumin-stained PE-A MPs increased from 0.003 mS cm^{-1} to 0.027 mS cm^{-1}, respectively. In contrast, the conductivity of the WW final effluent decreased upon spiking with curcumin-stained PE-A MPs from 0.925 mS cm^{-1} to 0.184 mS cm^{-1}, as Milli-Q water has very low ionic content. The negative surface charge of the virgin PE-A MPs was more pronounced because there were fewer counterions like Na^+, K^+, Fe^{2+}, NH_4^+, *etc.* to neutralize this negative charge. Curcumin-staining directly reduced the surface charge, leading to a noticeable drop in zeta potential, *i.e.*12 mV. Conversely, the WW final effluent contained various ions, dissolved salts and suspended organic matter. These particles can potentially reduce the electrical double layer around the PE-A MPs by masking the surface charge. As a result, curcumin-staining has a much lower reduction in zeta potential by 1.5 mV in the WW final effluent and is moderately stable.[23] Also, the reduced conductivity could enhance the electrophoretic mobility of MPs under an electric field. This is because a lower ionic strength reduced the shielding effect on the electric field, leading to more efficient movement of the MPs.

The microfluidic sensor developed by Rezai *et al.* in 2022[18] uses a DC electric field across two microwires inside a straight microchannel (150 μm × 200 μm) to generate an electrophoretic force to detect 1–10 μm polystyrene (PS) MPs at 5, 25 and 100 ppm concentrations. Compared to other microfluidic platforms, which often report detection limits in the range of 1–10 ppm, our sensor demonstrates improved sensitivity with a sub-ppm detection limit (0.825 ppm).[24] The study confirmed that the resistivity decreased with higher MP concentrations but showed limited sensitivity to 10 μm MPs compared to 1 and 5 μm-sized MPs. Therefore, this study extended the feasibility of the microfluidic sensor for detecting MPs smaller than 10 μm. A positive correlation was observed between MP concentration and the percentage reduction in normalized resistances for 1 and 5 μm MPs. Thus, in this study, we used the same microfluidic sensor and chose 10 ppm concentration for the detection of PE MPs of size 200–9900 nm (PE-A) at 10 ppm concentration. This can give a balance between being detectable and a manageable level in laboratory setup and simulating real-world scenarios. This concentration can be extrapolated to predict MP behaviour across various environmental scenarios.

The curcumin-stained PE-A MPs spiked in Milli-Q and the final effluent were run through the fabricated microfluidic device to analyze the resistance change upon accumulation around the anode. Fig. 3(A) shows the accumulation of curcumin-stained PE-A MPs in Milli-Q, while Fig. 3(B) shows accumulation in the WW final effluent at the anode of the microfluidic device. The accumulation trend for MPs based on size supported the previous findings on PS MPs.[18] A significant resistance drop was observed with lower-sized MPs *i.e.* 1 μm and 5 μm. In this study, as the curcumin-stained MPs were present in a broader size range (200–9900 nm), only smaller-sized ($\sim <500$ nm) MPs were captured at the anode and larger-sized MPs escaped through the channel. This demonstrates that the microfluidic device shows promising sensitivity for detecting smaller MPs (<500 nm), which are unaddressed so far, in environmental samples.

As observed in Table S8, the resistance dropped around 55% from the base resistance when curcumin-stained PE-A MPs were captured at the anode. However, with the WW final effluent, the resistance increased when PE-A MPs were captured at the anode of the microfluidic device. This increase was attributed to smaller organic particles present within the final effluent adhering to the copper electrodes. This reduced the effective conductive surface area around the anode, which led to an increase in the overall electrical resistance. Electrophoretic extraction of curcumin-stained PE-A MPs in the WW final effluent resulted in a positive normalized resistance (0.24 ± 0.03), whereas in Milli-Q water, the normalized resistance was negative (-0.55 ± 0.04), as shown in Fig. 3(C). The effect of the water matrix on the change in resistance was statistically significant as proved by Mann–Whitney *U* test with *p*-value $p < 0.0001$. This strongly highlighted the feasibility of the developed sensor in real-world scenarios such as the detection of MPs in WW and freshwater, among others.

This elaborate study on the novel approach of MP staining using an edible, biocompatible and biodegradable natural dye "curcumin" was successful. In addition, it also serves as an eco-friendly approach of MP staining by eliminating the production of secondary pollutants. Microscopic examination proved that curcumin produced a yellow stain on the surface of polyethylene microplastics, which produced green fluorescence under a fluorescence microscope (Fig. 3(b)). Curcumin potentially stained a wide population of different-sized PE MPs from 200–9900 nm and 180–212 μm efficiently elevating its applicability in real-time applications. The stained MPs can be recovered by destaining using methanol, proving that only electrostatic interactions exist between

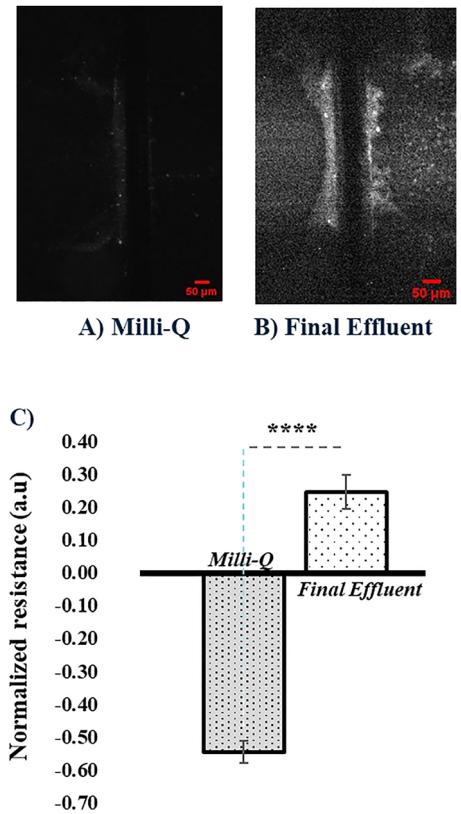

Fig. 3 Accumulation of curcumin-stained PE-A MPs around the anode after 10 minutes (A) in Milli-Q and (B) final effluent and (C) normalized resistance at 10 ppm concentration. Error bars are SD. ****: $p < 0.0001$.

the PE MPs and curcumin. This was further justified by Fourier transform Infrared spectroscopic analysis where the characteristic peaks of virgin PE MPs were retained after curcumin-staining. Curcumin is neutral at pH 7 to 8, which favours staining of MPs in WW and freshwaters. Thus, curcumin-staining proves to be an excellent, novel and eco-friendly approach for fluorescence-based detection of MPs that simultaneously promotes sustainable development goals. The resistance measurements showed (Fig. 3(c)) a positive normalized resistance of 0.24 ± 0.03 in the WW final effluent, while the normalized resistance of Milli-Q was at -0.55 ± 0.04. Fluorescence microscopy showed the accumulation of the smaller-sized PE-A MPs (<500 nm) from the wide size range used. This strongly indicates the feasibility of the simple microfluidic device that used a DC electric signal to detect the unaddressed size range of MPs in environmental matrices. However, for real-world applications, pretreating water samples before detection inside a microfluidic sensor is essential. Chemical pretreatment can lead to degradation of the microfluidic device with time. Thus, ultrasonication and filtration using a 10 µm pore-sized filter prior to running a water sample through the sensor can potentially remove all the larger particles and prevent blockage of the microfluidic channel. Incorporating a spectroscopic analytical technique can distinguish among the different types of MPs being accumulated at the anode. Thus, the sensor needs to be modified to make it more sensitive and efficient towards different environmental samples such as raw WW, seawater *etc.* Overall, this study establishes a proof-of-concept for curcumin staining as a promising ecofriendly strategy for the simultaneous optical and electrical detection of MPs. Future research will focus on further optimizing the workflow, extending its applicability to diverse environmental samples, and advancing towards a robust MP detection system.

Juviya Mathew: methodology, investigation, data curation, formal data analysis, visualization, writing – original draft, writing – review and editing; Haider Warraich: methodology, investigation, data curation, formal data analysis, visualization, writing – original draft, writing – review and editing; Ratul Kumar Das: conceptualization, methodology, visualization, validation, supervision, writing – original draft, writing – review and editing; Pouya Rezai: conceptualization, project administration, supervision, validation, writing review and editing and resources; Satinder Kaur Brar: conceptualization, project administration, supervision, funding, writing – review and editing and resources.

This research was funded by the Natural Sciences and Engineering Research Council (Discovery Grant 23451, NSERC Alliance Option-2 Grants MISSED Project, ALLRP 571066-21). We would also like to thank James and Joanne Love Chair in Environmental Engineering for their financial support. We would also like to thank Sejal Dave and Prof. Raymond Kwong, Department of Biology, York University, for their valuable support and guidance in using the microscope for fluorescence studies.

Conflicts of interest

There are no conflicts to declare.

Data availability

The data supporting this article have been included as part of the SI. See DOI: https://doi.org/10.1039/d5cc02304a.

Notes and references

1 Y.-N. Chen, *et al.*, *Environ. Technol. Innovation*, 2023, **32**, 103250.
2 J. Mathew, *et al.*, *J. Water Proc. Eng.*, 2024, **64**, 105702.
3 A. A. Horton and S. J. Dixon, *WIREs Water*, 2018, **5**, e1268.
4 M. S. M. Al-Azzawi, *et al.*, *Sci. Total Environ*, 2023, **863**, 160947.
5 L. Nalbone, *et al.*, *Mar. Pollut. Bull.*, 2021, **172**, 112888.
6 F. Ribeiro, *et al.*, *TrAC, Trends Anal. Chem.*, 2024, **172**, 117555.
7 M. T. Sturm, *et al.*, *Sci. Total Environ*, 2022, **806**, 151388.
8 A. L. Andrady, Proceedings of the Second Research Workshop on Microplastic Marine Debris, NOAA Tech, Memo 54, 2010.
9 T. Maes, *et al.*, *Sci. Rep.*, 2017, **7**, 44501.
10 T. Matthias, *J. Earth Sci. Environ. Stud.*, 2017, **2**, DOI: 10.15436/jeses.2.2.1.
11 G. Malafaia, *et al.*, *J. Hazard. Mater. Adv.*, 2022, **6**, 100054.
12 Search | FDA, https://www.fda.gov/search?s=curcumin, (accessed February 7, p. 2025).
13 R. K. Das, *et al.*, *Nanomedicine*, 2010, **6**, 153–160.
14 D. Patra and C. Barakat, *Spectrochim. Acta, Part A*, 2011, **79**, 1034–1041.
15 S. J. Hewlings and D. S. Kalman, *Foods*, 2017, **6**, 92.
16 J. A. DePasquale, *Photochem. Photobiol. Sci.*, 2024, **23**, 1893–1914.
17 P. Wu, *et al.*, *Anal. Chem.*, 2020, **92**, 14346–14356.
18 A. Zabihihesari, *et al.*, *New J. Chem.*, 2023, **47**, 9050–9060.
19 S. Jasim, *AACE Clin. Case Rep.*, 2021, **7**, 1.
20 N. Safie, *et al.*, *Malays. J. Anal. Sci.*, 2015, **19**, 1243–1249.
21 J. V. Gulmine, *et al.*, *Polym. Test.*, 2002, **21**, 557–563.
22 K. I. Priyadarsini, *J. Photochem. Photobiol., C*, 2009, **10**, 81–95.
23 Zeta Potential – Overview, https://www.malvernpanalytical.com/en/products/measurement-type/zeta-potential, (accessed October 29, 2024).
24 H. Warraich, *et al.*, *Microchim. Acta*, 2025, **192**, 476.